Study of the post-annealing effect for the MoSi$_2$ compound

J. H. Seo^a, Y. S. Lee^{a,}*, M. S. Jeon^b, J. K. Song^b, C. W. Jeong^c, D. B. Han^c and S. K. Rha^d
^{a}Department of Information Communication Engineering, Hanbat National University, Daejon 305-719
^{b}Material Analysis Team Machinery & Material Center, Korea Testing Laboratory, Seoul 222-13
^{c}Winner Technology Co., LTD. 581-17, Geumgok-Ri, Anjung-Eup, Pyongtaek City
^{d}Department of Materials Engineering, Hanbat National University, Daejon 305-719

The low-temperature oxidation of the MoSi$_2$ compound prepared by a self-propagating high temperature synthesis (SHS) reaction from a mixture of Mo and Si powders has been investigated by comparing the structural and chemical destructions of the MoSi$_2$ compound. One of the comparable samples was a pellet sintered at 1700 °C and the other was synthesized powder annealed at 400 °C in air. The phase structure, microstructures, and chemical states of the samples were measured by XRD, SEM, and XPS. From the results of the analysis, the powder synthesized by SHS had a body-centred tetragonal MoSi$_2$ crystal structure together with SiO$_2$ and MoO$_3$ amorphous phases from air contamination, the sample sintered at 1700 °C had a similar crystal structure to synthesized powder. On the other hand, the crystal structure of the powder annealed at 400 °C was destroyed completely into amorphous SiO$_2$ and crystalline MoO$_3$ phases and the loss of Mo content occurred by volatilizing MoO$_3$.

Key words: MoSi$_2$, Self-propagating high temperature synthesis, Oxidation, XRD, XPS.

Introduction

Molybdenum disilicide (MoSi$_2$) is an attractive high temperature structural material due to a high melting point, high hardness and good oxidation resistance compared with other refractory silicides and intermetallic compounds. Nevertheless, there are many problems in the use of MoSi$_2$ according to the temperature range; at ≤ 800 K, the structural destruction of MoSi$_2$ when a MoSi$_2$ construction is exposed to air.; low ductility and lack of plasticity below 1273-1473 K (brittle-to-ductile transition temperature); inadequate strength and creep resistance above 1573 K [1-3]. However, there are still critical issues which remain to be resolved for its use. In particular, a full understanding of the structural destruction is required because the structural destruction by oxidation at low temperature is one of catastrophic problems in applications. The details of the structural destruction are not sufficiently clear as yet.

In the present study, we attempted to fabricate MoSi$_2$ compound by a self-propagating high temperature synthesis (SHS) reaction from a mixture of Mo and Si powders. It is known that SHS is a method in which materials with a high melting point are fabricated by combustion of reactant powders with a large exothermic heat output at a low temperature and low pressure in a short time and so the cost may be relatively low [2, 4, 5]. In order to understand the structural destruction of MoSi$_2$ compounds as oxidation

resistance materials, we investigated the phase structure, microstructures and chemical states of the compounds.

Experiments

Mo (Chengdu Hongbo Inductrial Co. Ltd, purity 99.95%) and Si (CW Co. Ltd, purity 99.95%) powders were mixed in the desired ratio (atomic ratio of Mo/Si = 1/2). The mixtures were ball-milled for 15 h using Al$_2$O$_3$ balls. Pellets were formed by compression of the as-milled powder (150 kg/cm^2) and the pellet size was 96 × 50 mm before the SHS procedure. The pellet was placed in a reaction chamber under an atmosphere of high purity H$_2$ to minimize the oxidation of the powder during SHS reaction. The preheating of the pellet was carried out to 700 °C prior to ignition.

The SHS reaction was ignited by heating the upper surface of the pellet using a tungsten wire. The reaction time was ~ 1 minute. The reaction product was cooled to ambient temperature in the chamber, was broken into fragments (≤ 3 mm), and ground by Al$_2$O$_3$ ball milling for 15 h. Subsequently, the ground powders were sieved through a 200-mesh sieve. In order to obtain powder with a particle size of ≤ 10 μm, the sieved powders with a particle size below 74 μm further ground at 137 rpm for ~ 50 minutes by attrition milling using ZrO$_2$ balls and ethanol. In addition, the resultant product was dried in an oven at 80 °C for at least 24 h. Finally, in order to obtain an agglomerate-free powder, a pin mill was used.

In order to understand the structural destruction, we compared a pellet sintered at 1700 °C with a powder annealed at 400 °C. The sintered pellet was made as follows;

*Corresponding author:
 Tel : +82-42-821-1148
 Fax: +82-42-821-1595
 E-mail: yslee@hanbat.ac.kr

the final powder formed by SHS was kneaded with an organic binder, the kneaded powder was compressed again into a pellet of diameter 6 mm, and this pellet was sintered at 1700 °C in air. In addition, an annealed powder was obtained by the annealing of the synthesized final powder at 400 °C in air for 12 h.

The reaction products were analyzed using a scanning electron microscope (SEM, Hitachi, Japan, Model S-25OOC) and an X-ray Diffractometer (XRD, Rigaku, Japan, Model M/Max-IIIA). The chemical states of the composites were investigated by X-ray photoelectron spectroscopy (XPS, VG ESCA LAB 210) using an Al Kα source.

Results and Discussion

Fig. 1 shows the XRD patterns for the samples. For the synthesis of the powder with $MoSi_2$ phase, Mo powder with the typical cubic (space group *Im3m* : no.229) crystal structure [6] was mixed with Si powder using the SHS method in Fig. 1(a) and 1(b). As shown in Fig. 1(a) and 1(b), other phases such as unreacted Mo and Si and other Mo-silicides (Mo_3Si and Mo_5Si_3 etc. [7-9]) were not detected. The crystal structures of the synthesized powder of Fig. 1(c) and the pellet of Fig. 1(d) are typical body-centred tetragonal (bct) $MoSi_2$ (space group *I4/mmm* : no.139). By comparison with the synthesized $MoSi_2$ powder, the intensity

of the XRD peaks for the pellet sintered in air at 1700 °C decreases overall and the background of lower 2-theta is higher. In general, this higher background means an amorphization of the sample. After sintering at a high temperature 1700 °C for the synthesized $MoSi_2$ powder, the crystal structure was still bct. However, after annealing the synthesized $MoSi_2$ powder at lower temperature, 400 °C, the XRD pattern was changed completely; the $MoSi_2$ phase disappeared and the MoO_3 phase (space group *Pbnm* : no.62) appeared.

Fig. 2 shows SEM images for samples. As shown in Fig. 2(a) and 2(b), the SEM images for the synthesized powder and the pellet sintered at 1700 °C are similar.
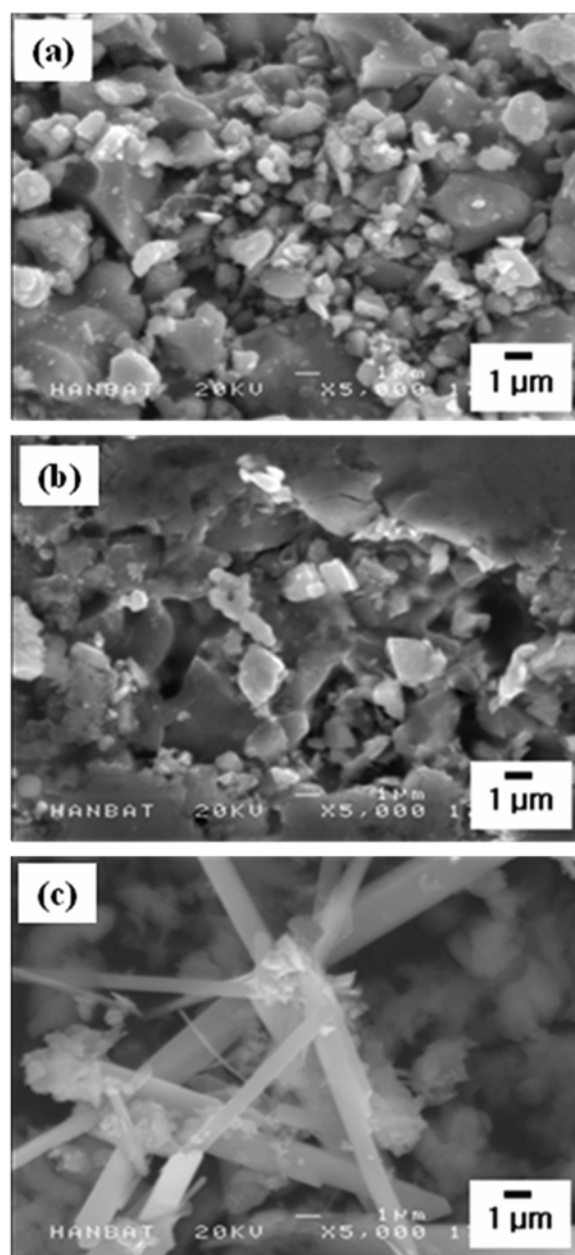
Fig. 2. SEM images for (a) the synthesized $MoSi_2$ powder, (b) the $MoSi_2$ pellet pressed with an organic binder and sintered in air at 1700 °C and (c) the $MoSi_2$ powder oxidized in air at 400 °C.

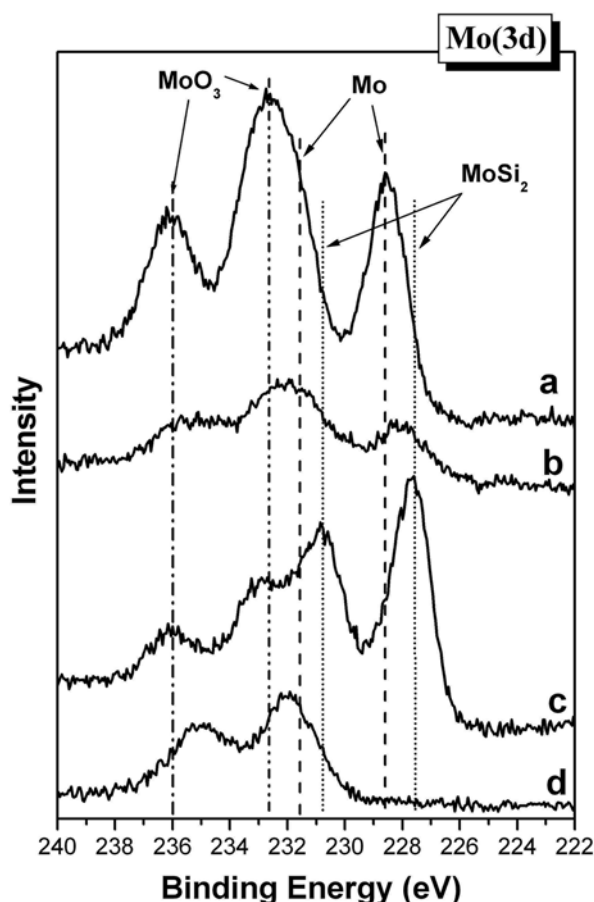**Fig. 1.** XRD patterns for (a) Mo and (b) Si source materials, (c) the synthesized $MoSi_2$ powder, (d) the $MoSi_2$ pellet pressed with an organic binder and sintered in air at 1700 °C and (e) the $MoSi_2$ powder oxidized in air at 400 °C.

This result agrees well with the XRD results that both powders have the same crystal structure. However, the SEM image for the powder annealed at 400 °C changed abruptly. We can see the sharp rod type structure as shown in Fig. 2(c). From the XRD result, we can expect that the rods are composed of MoO_3.

Fig. 3 shows the Mo (3d) XPS spectra for the Mo source powder, synthesized alloy powder, pellet sintered at 1700 °C and powder annealed at 400 °C. For the Mo source powder [Fig. 3(a)], three peaks are seen; the peak of the binding energy at 228.6 eV corresponds to $3d_{5/2}$ of metallic Mo; the broad peak at 232.7 eV formed by overlap of $3d_{3/2}$ (231.8 eV) of metallic Mo and $3d_{5/2}$ (232.85 eV) of MoO_3; the peak at 236.1 eV of the highest binding energy corresponded to $3d_{3/2}$ of MoO_3 [10]. We can see that the source Mo powder already contains some amounts of MoO_3 due to the exposure to air. After synthesis by SHS, the peaks in Fig. 3(b) shifted to lower binding energies. In the pellet sample sintered at 1700 °C [Fig. 3(c)], four peaks are clearly observed and the peaks at 227.6 eV and 230.8 eV increase abruptly. These peaks at 227.6 eV and 230.8 eV correspond to $MoSi_2$ $3d_{5/2}$ and $3d_{3/2}$ peaks, respectively [10]. From

these results, it seems that the synthesized alloy powder contains several phases ($MoSi_2$, Mo oxides, and metallic Mo). However, the metallic Mo and the Mo oxides were not detected in the XRD pattern [Fig. 1(c)]. The Mo-oxide peaks cannot be detected in the XRD patterns because Mo oxides formed by air contamination have an amorphous structure. However, if metallic Mo unreacted with Si exists, the metallic Mo peaks such as in Fig. 1(a) must appear. Therefore, we can suggest that the $MoSi_2$ phase forms with Mo-oxides by SHS. From the results, after sintering at 1700 °C, the formation of the $MoSi_2$ phase is obviously more. In addition, for the sample annealed at 400 °C in Fig. 3(d), the peak at ~ 228 eV disappears and just double peaks assigned to MoO_3 are observed. The binding energy of these double peaks is lower than that from MoO_3 by air contamination. This lower shift may be due to the MoO_3 with the crystal structure as shown in Fig. 1(e).

Fig. 4 shows the Si (2p) XPS spectra. The source Si powder contains SiO_2 by air contamination [Fig. 4(a)]; peaks at 99 eV and 103.3 eV correspond to elemental Si and SiO_2, respectively [10]. As shown in Fig. 4(c) and 4(d), the $MoSi_2$ phase (99.2 eV [10]) for the pellet

Fig. 3. Mo (3d) XPS spectra for (a) Mo source materials, (b) the synthesized MoSi₂ powder, (c) the MoSi₂ pellet pressed with an organic binder and sintered in air at 1700 °C and (d) the MoSi₂ powder oxidized in air at 400 °C.
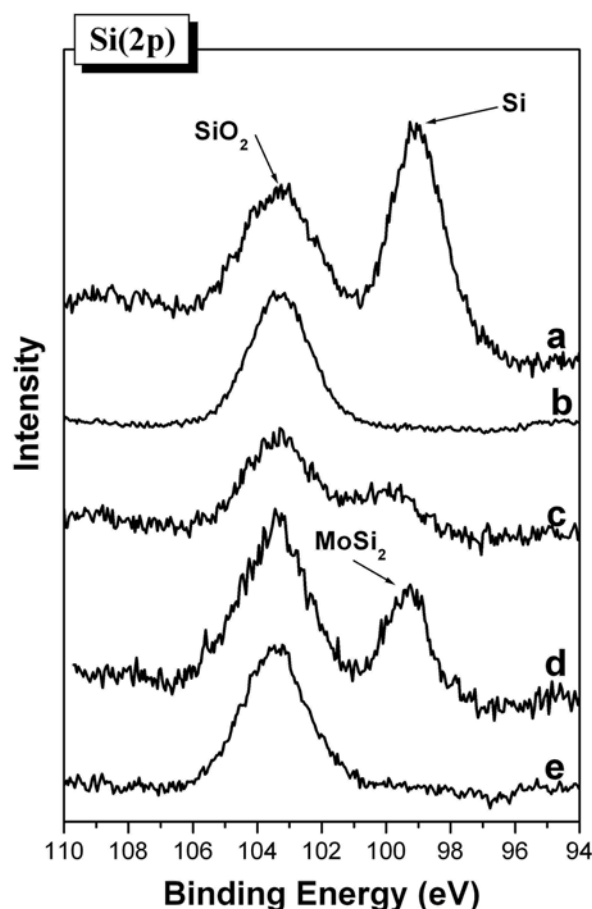
Fig. 4. Si (2p) XPS spectra for (a) Si source material, (b) SiO₂ powder, (c) the synthesized MoSi₂ powder, (d) the MoSi₂ pellet pressed with an organic binder and sintered in air at 1700 °C and (e) the MoSi₂ powder oxidized in air at 400 °C.

8. G. Cabouro, S. Chevalier, E. Gaffet, D. Vrel, N. Boudet and F. Bernard, Acta Mater. 55 (2007) 6051-6063.
9. B.K. Yen, T. Aizawa and J. Kihara, Mater. Sci. Eng. A220 (1996) 8-14.
10. J.F. Moulder, W.F. Stickle, P.E. Sobol and K.D. Bomben, in "Handbook of X-ray Photoelectron Spectroscopy" (Physical Electronics Inc., USA, 1995).
11. G.H. Aylward and T.J.V. Findlay, in "SI Chemical Data"
(Joh Wiley & Sons Australasia PTY. LTD., Syney, 1971) p.47 and p.59.
12. O. Kubaschewski, C.B. Alcock and P.J. Spencer, in "Materials Thermo-chemistry" (Pergamon, Oxford, 1993).
13. L. Peiqing, X. Qunji and L. Weimin, Surface and Coatings Tech. 135 (2001) 118-125.
14. M. Chase, in "Binary Alloy Phase Diagrams" 2nd Edi. (ASM International, Materials Park, Ohio, 1996).